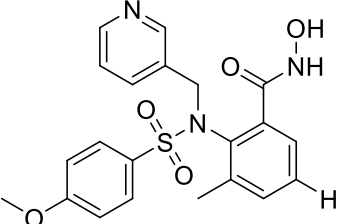
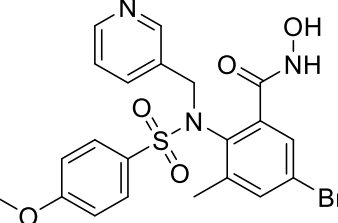
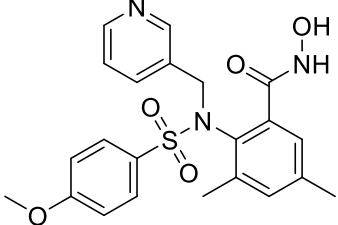
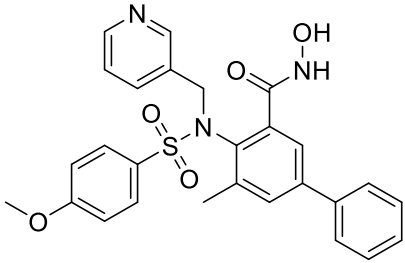
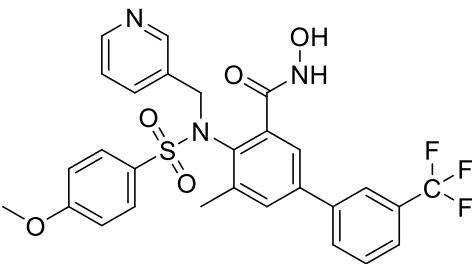
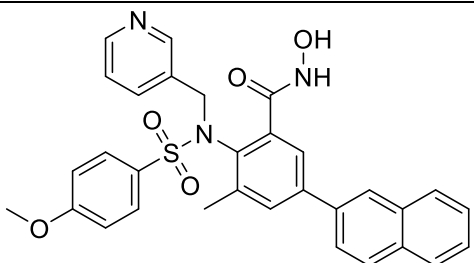
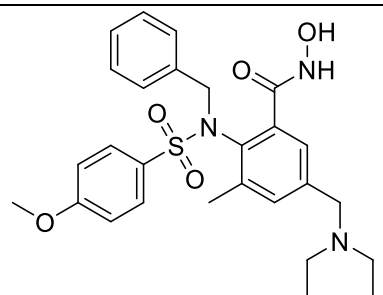


Supplementary Data

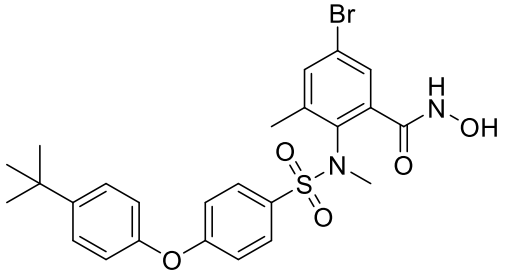
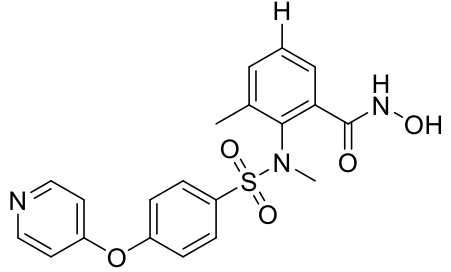
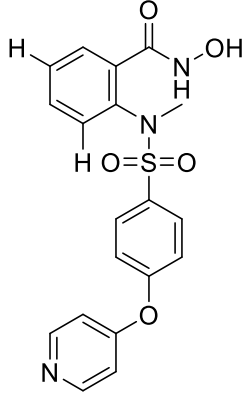
Table S1. Chemical structures for the data set of 67 compounds with corresponding pIC_{50} values.

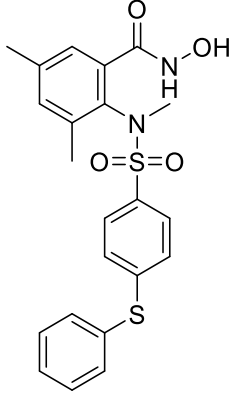
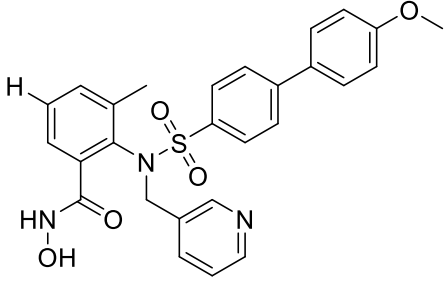
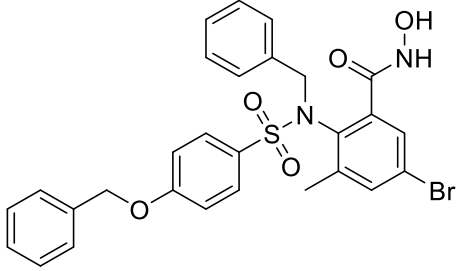
Compound	Structure	IC ₅₀ (μ M)	pIC_{50}	Predicted activity	Residual Factor	References
1		0.005	8.30103	7.60352	-0.697507	J. Levin, et al., 2001;
2		0.024	7.619789	7.70339	0.0835988	J. Levin, et al., 2001;
3		0.015	7.823909	7.68744	-0.136468	J. Levin, et al., 2001;

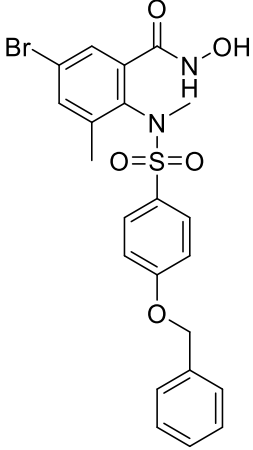
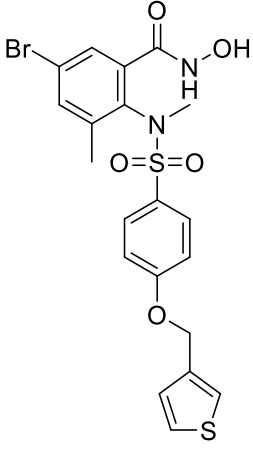
4		0.003	8.522879	8.5737	0.0508204	J. Levin, et al., 2001;
5		0.001	9	8.78496	-0.215042	J. Levin, et al., 2001;
6		0.002	8.69897	8.80159	0.102623	J. Levin, et al., 2001;
7		0.005	8.30103	8.35062	0.0495947	J. Levin, et al., 2001;

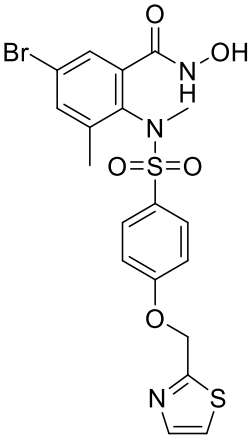
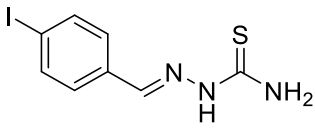
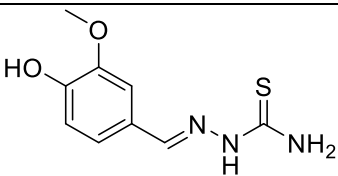
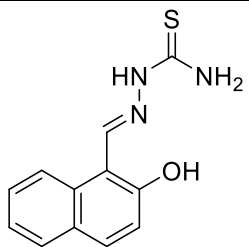
8		0.002	8.69897	7.99622	-0.70275	J. Levin, et al., 2001;
9		0.007	8.154902	8.19562	0.0407221	J. Levin, et al., 2001;
10		0.008	8.09691	7.82786	-0.269048	J. Levin, et al., 2001;

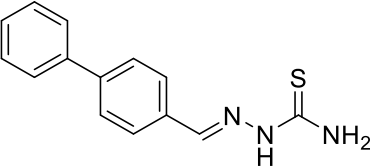
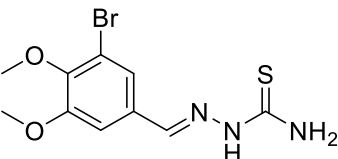
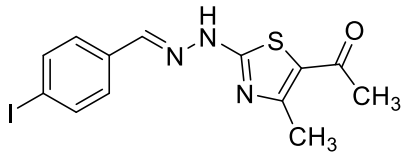
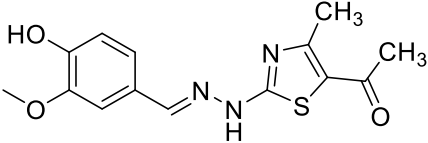
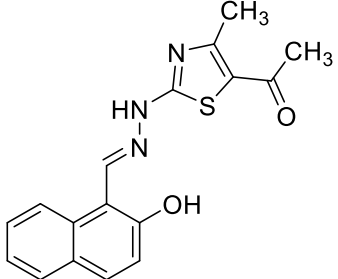
11		0.144	6.841638	6.91105	0.0694115	J. Levin, et al., 2001;
12		0.554	6.25649	-	-	J. Levin, et al., 2001;
13		0.046	7.337242	7.25829	-0.0789566	J. Levin, et al., 2001;
14		0.004	8.39794	8.1804	-0.217541	J. Levin, et al., 2001;

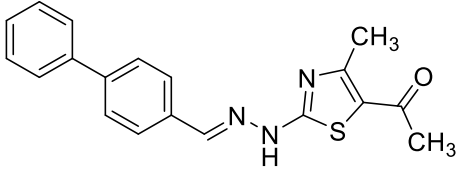
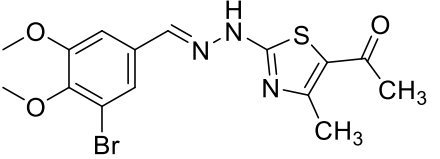
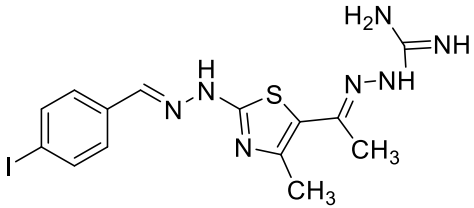
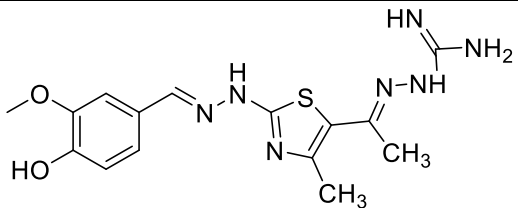
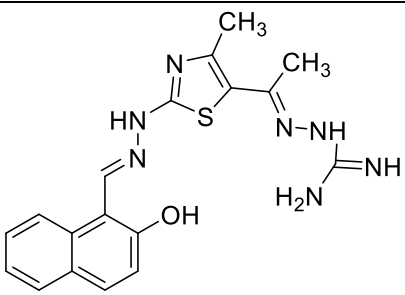
15		0.125	6.90309	6.9712	0.0681133	J. Levin, et al., 2001;
16		0.007	8.154902	8.11264	-0.042267	J. Levin, et al., 2001;
¹⁷		0.153	6.815309	6.63392	-0.181385	J. Levin, et al., 2001;

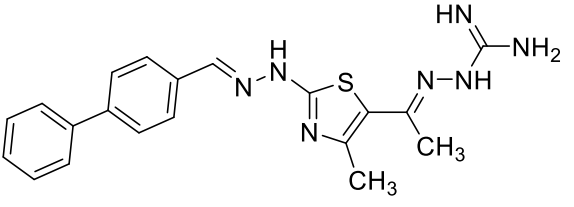
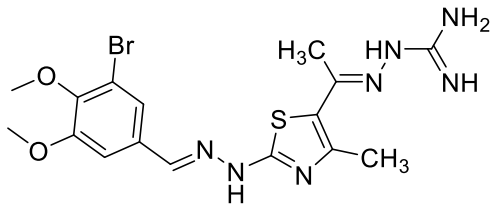
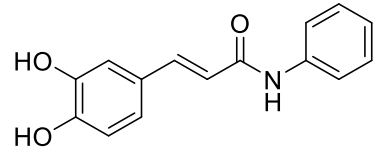
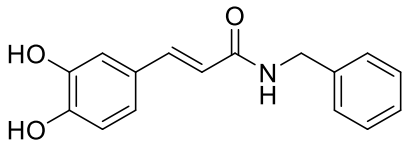
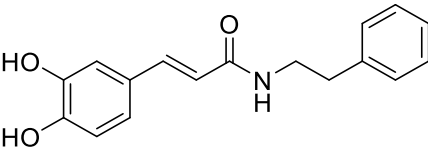
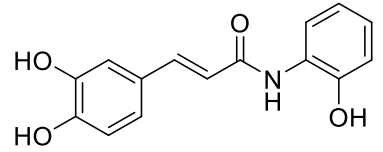
¹⁸		0.008	8.09691	7.71709	-0.379818	J. Levin, et al., 2001;
¹⁹		0.152	6.818156	6.557	-0.261154	J. Levin, et al., 2001;
20		3.448	5.462433	5.58179	0.119359	J. Levin, et al., 2001;

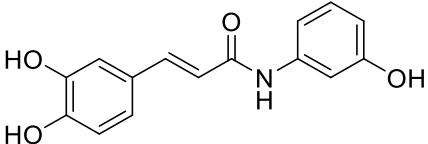
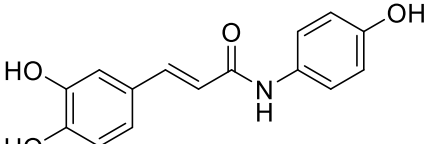
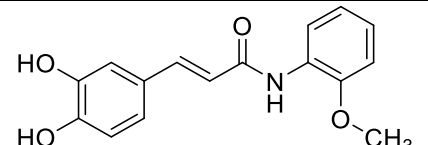
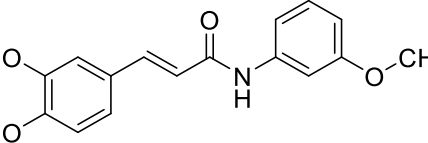
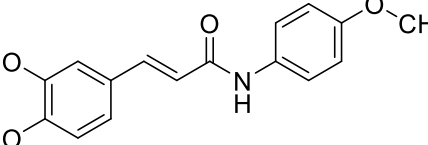
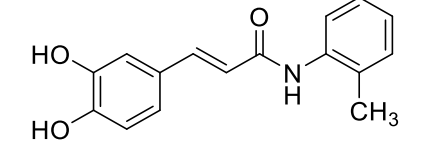
21		0.189	6.723538	6.6892	-0.0343412	J. Levin, et al., 2001;
'22		0.232	6.634512	6.65487	0.020357	J. Levin, et al., 2001;

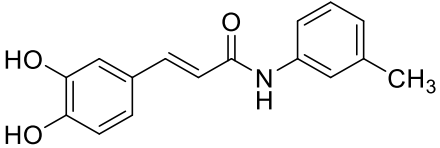
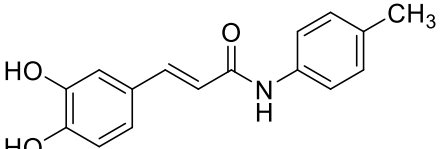
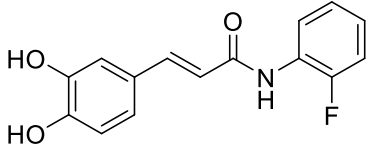
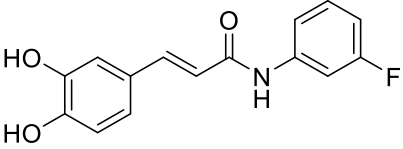
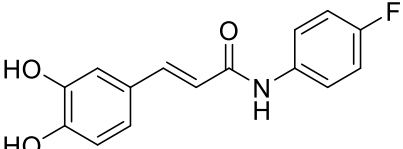
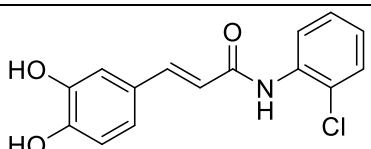
23		0.952	6.021363	6.12075	0.0993916	J. Levin, et al., 2001;
24		0.59004	6.229119	6.4716	0.242483	Omar et al., 2020
25		0.10582	6.975432	6.83941	-0.13602	Omar et al., 2020
26		0.07611	7.118558	6.39433	-0.724229	Omar et al., 2020

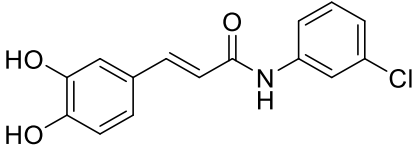
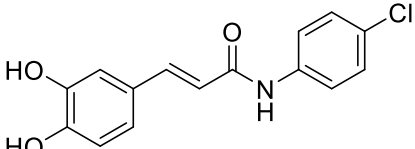
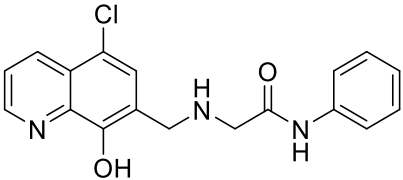
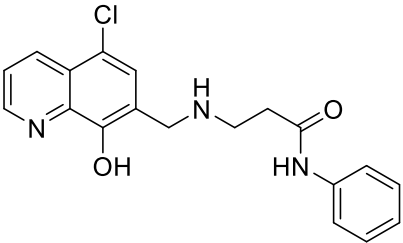
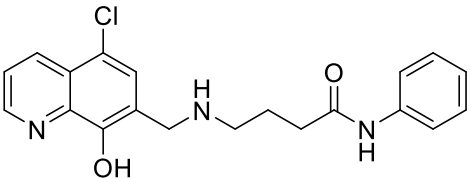
^t 27		0.09434	7.025304	7.09946	0.0741556	Omar et al., 2020
^t 28		0.10917	6.961897	6.95577	-0.00612625	Omar et al., 2020
29		0.35890	6.445027	6.68998	0.24495	Omar et al., 2020
^t 30		0.02093	7.679231	7.32964	-0.349596	Omar et al., 2020
31		0.02877	7.54106	7.40491	-0.13615	Omar et al., 2020

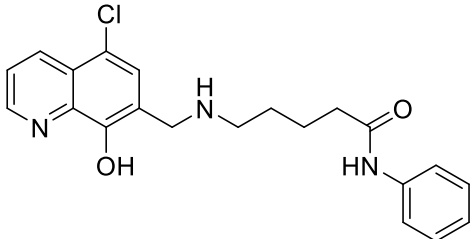
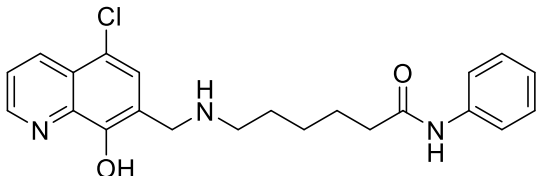
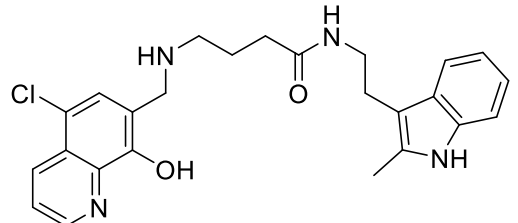
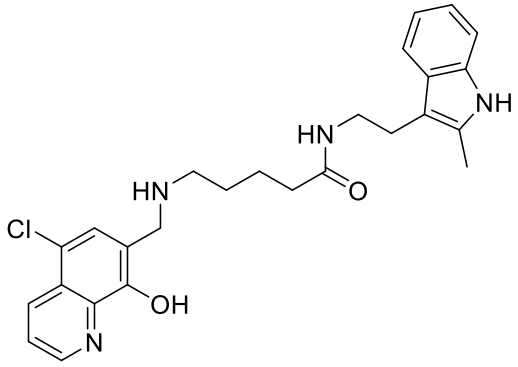
32		0.13807	6.859901	6.81372	-0.0461788	Omar et al., 2020
33		0.13792	6.860373	6.94409	0.0837131	Omar et al., 2020
34		0.03860	7.413413	7.44445	0.0310361	Omar et al., 2020
35		0.06233	7.205303	-	-	Omar et al., 2020
36		0.08605	7.065249	7.25206	0.186812	Omar et al., 2020

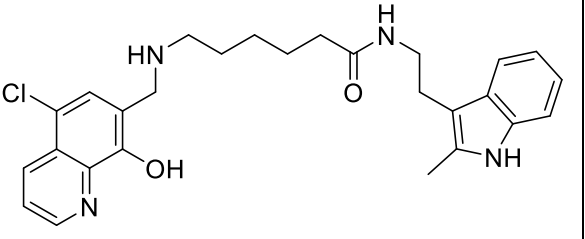
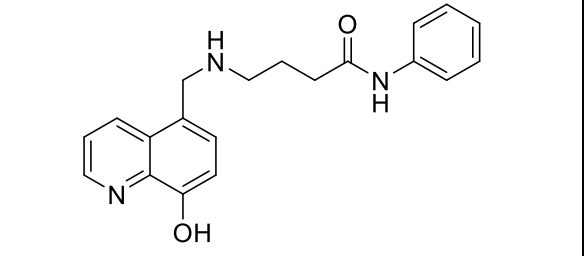
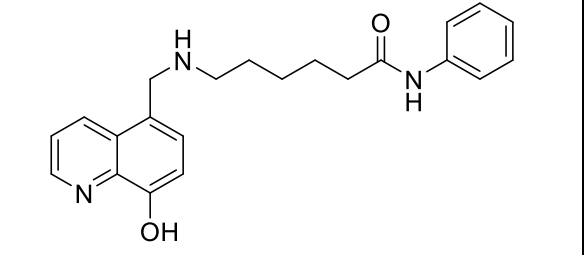
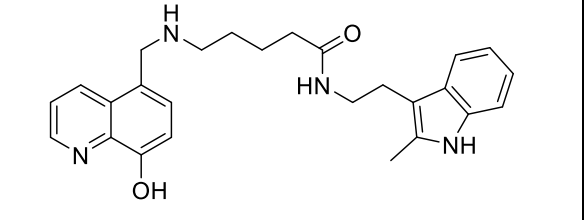
37		0.05687	7.245117	7.37439	0.129269	Omar et al., 2020
38		0.06433	7.191586	7.45972	0.268132	Omar et al., 2020
39		0.00714	8.146302	7.9581	-0.188206	Shi et al., 2012
40		0.00725	8.139662	-	-	Shi et al., 2012
^t 41		0.00728	8.137869	7.6597	-0.478091	Shi et al., 2012
^t 42		0.00528	8.277366	7.83931	-0.438057	Shi et al., 2012

43		1.64227	5.784555	6.4691	0.684549	Shi et al., 2012
^t 44		0.00235	8.628932	7.90856	-0.720371	Shi et al., 2012
45		0.00567	8.246417	8.51253	0.266114	Shi et al., 2012
46		1.63242	5.787168	-	-	Shi et al., 2012
47		0.00333	8.477556	8.57493	0.0973757	Shi et al., 2012
48		0.00591	8.228413	7.23113	-0.997286	Shi et al., 2012

^t 49		1.75385	5.756008	6.56691	0.180902	Shi et al., 2012
^t 50		0.00364	8.438899	8.13051	-0.308392	Shi et al., 2012
51		0.00781	8.107349	8.18479	0.0774371	Shi et al., 2012
52		1.86959	5.728254	-	-	Shi et al., 2012
53		0.00729	8.137272	7.07264	-1.06464	Shi et al., 2012
54		0.00819	8.086716	8.28299	-0.196272	Shi et al., 2012

55		1.92113	5.716443	6.55879	0.842346	Shi et al., 2012
56		0.00789	8.102923	8.1758	0.072873	Shi et al., 2012
57		2.1	5.677781	5.6568	-0.0209825	C. Chen et al., 2019
58		3.5	5.455932	5.20299	-0.252947	C. Chen et al., 2019
59		3.2	5.49485	5.71479	0.219938	C. Chen et al., 2019

60		3.6	5.443697	5.35485	-0.0888422	C. Chen et al., 2019
61		0.66	6.180456	6.38792	0.207467	C. Chen et al., 2019
62		1.3	5.886057	5.75928	-0.12678	C. Chen et al., 2019
63		3.1	5.508638	-	-	C. Chen et al., 2019

64		1.7	5.769551	-	-	C. Chen et al., 2019
^t 65		5.1	5.29243	5.95646	0.664032	C. Chen et al., 2019
^t 66		6.0	5.221849	6.0173	0.79545	C. Chen et al., 2019
67		5.3	5.275724	5.13355	-0.142178	C. Chen et al., 2019

t: test ligands

Table S2a. Angles between different sites of model DDHRR_1.

Site1	Site2	Site3	Angles (Å)
H9	R13	R14	68.0
H9	D7	R14	37.4
D8	R13	H9	21.8
D8	D7	R14	58.8
R13	D8	R14	34.7
H9	D7	R14	83.7

Table S2b. Distances between different sites of model DDHRR_1.

Site 1	Site 2	Distance (Å)
H9	R13	2.89
R13	R14	6.19
D8	H9	5.85
D7	D8	2.09
R14	D7	4.70
R14	D8	4.93
H8	D7	7.69

D8	R13	3.53
H8	R14	6.67

Table S3. Results of Y-Scrambling method

Model	R	R²
Original	0.504724	0.254747
Random 1	0.324377	0.10522
Random 2	0.417006	0.173894
Random 3	0.285357	0.081428
Random 4	0.306254	0.093791
Random 5	0.27919	0.077947
Random 6	0.226197	0.051165
Random 7	0.162422	0.026381
Random 8	0.396729	0.157394
Random 9	0.176174	0.031037
Random 10	0.334835	0.112115

Random Model Parameters

Average r: 0.290854

Average r^2 : 0.091037

Average Q^2 : -0.18697

cRp²: 0.208195

Table S4. Results of Xternal Validation Plus 1.1 tool using mean absolute error-based criteria.

User Input File Information	File Name	Values
Model biasness test	nPE/nNE	1.7632
	nNE/nPE	0.5672
	MPE/MNE	1.1445
	MNE/MPE	0.8738
	AAE- AE	0.2669
	R ²	0.8936
Error-based metric (after removing 5% data with high residues)	MAE (95% data)	0.3734
	MAE+3×SD (95% data)	1.1394
Threshold values utilized to judge the model predictions	0.1×training set range	0.7820
	0.15×training set	1.1729

	range	
	0.2×training set range	1.5639
	0.25×training set range	1.9549
Result (MAE-based criteria applied on 95 % data)	Prediction quality	GOOD

Table S5. Molecular docking results (kcal/mol) of phase data set ligands **1-67** showing interacting amino acids.

S. No	^a Gscore	^b GvdW	^c Genergy	^d Gemodel	^e Gecolumb
1	-4.493	-35.663	-41.291	-48.185	-5.628
2	-6.087	-41.593	-46.242	-67.45	-4.649
3	-4.779	-34.092	-41.765	-55.184	-7.673
4	-4.389	-39.805	-46.79	-61.051	-6.985
5	-8.414	-43.328	-51.7	-72.803	-8.373
6	-5.401	-49.594	-53.257	-74.4	-3.663
7	-4.389	-36.927	-41.84	-55.63	-4.913
8	-2.791	-41.163	-46.258	-60.254	-5.096
9	-4.132	-34.412	-40.397	-52.98	-5.985
10	-3.526	-36.049	-45.256	-60.5	-9.207

11	-4.751	-44.741	-45.189	-65.173	-0.448
12	-7.195	-44.505	-55.486	-82.218	-10.981
13	-6.799	-52.335	-60.828	-94.659	-8.493
14	-7.265	-45.047	-55.406	-78.652	-10.359
15	-6.312	-57.287	-64.482	-73.201	-7.195
16	-5.912	-50.396	-57.617	-83.664	-7.222
17	-6.166	-52.536	-61.48	-88.346	-8.944
18	-5.095	-52.904	-59.001	-81.513	-6.098
19	-6.787	-53.252	-58.153	-82.969	-4.9
20	-7.343	-54.414	-56.25	-80.945	-1.836
21	-5.936	-52.24	-61.083	-96.14	-8.844
22	-4.584	-54.017	-64.018	-95.315	-10.001
23	-3.851	-56.463	-65.78	-98.708	-9.318
24	-6.563	-33.545	-38.952	-48.513	-5.407
25	-7.532	-34.057	-43.193	-59.701	-9.136
26	-5.5	-29.901	-36.838	-51.539	-6.937
27	-7.702	-41.849	-45.831	-69.613	-3.982
28	-5.954	-34.965	-39.445	-41.239	-4.481
29	-6.846	-46.413	-48.655	-68.093	-2.242
30	-7.682	-48.108	-52.637	-68.972	-4.53
31	-7.761	-37.77	-45.449	-71.019	-7.679

32	-6.842	-51.294	-53.614	-83.242	-2.32
33	-6.973	-44.881	-48.464	-59.131	-3.583
34	-6.448	-45.367	-51.147	-74.571	-5.78
35	-7.553	-55.159	-59.287	-73.504	-4.128
36	-7.62	-48.417	-54.541	-74.375	-6.124
37	-7.223	-54.469	-56.358	-93.305	-1.889
38	-7.067	-54.874	-59.57	-76.49	-4.697
39	-7.178	-42.102	-44.041	-67.234	-1.939
40	-7.476	-41.425	-44.614	-62.875	-3.189
41	-7.454	-43.286	-48.655	-70.255	-5.37
42	-7.816	-40.961	-47.845	-72.853	-6.884
43	-7.531	-40.808	-48.562	-75.11	-7.754
44	-8.072	-43.635	-51.677	-78.469	-8.042
45	-6.927	-46.31	-48.802	-64.097	-2.492
46	-6.701	-45.752	-48.664	-69.289	-2.913
47	-7.611	-44.315	-49.863	-72.365	-5.548
48	-6.765	-43.78	-46.752	-65.176	-2.972
49	-6.759	-44.079	-46.503	-63.753	-2.424
50	-6.782	-44.506	-46.912	-66.459	-2.405
51	-6.891	-42.269	-44.507	-61.136	-2.238
52	-7.229	-42.317	-44.162	-65.048	-1.846

53	-7.016	-43.541	-47.713	-64.85	-4.172
54	-6.979	-45.279	-47.737	-63.676	-2.457
55	-7.301	-45.105	-48.33	-68.302	-3.226
56	-7.036	-45.035	-47.4	-68.71	-2.366
57	-6.84	-42.235	-49.306	-70.372	-7.071
58	-7.507	-45.853	-53.795	-80.82	-7.942
59	-8.023	-44.255	-53.776	-80.301	-9.521
60	-8.504	-46.704	-58.246	-87.615	-11.542
61	-8.33	-51.345	-61.586	-91.363	-10.241
62	-5.16	-38.282	-46.498	-64.594	-8.216
63	-7.175	-45.89	-48.729	-68.25	-2.84
64	-7.629	-43.939	-50.158	-72.322	-6.219
65	-7.108	-46.161	-50.501	-71.562	-4.34
66	-5.072	-26.841	-45.035	-61.459	-5.194
67	-7.749	-52.571	-56.506	-71.758	-3.935

^aglide score; ^bglide Van der Waal; ^cglide energy; ^dglide Emodel; ^eglide Ecolumb.

Table S6. Binding free energy (MM-GBSA) calculation (kcal/mol) of data set ligands **1-67**.

S. No	^a ΔG_{bind}	^b ΔG_{coul}	^c ΔG_{cov}	^c ΔG_{Hbond}	^d ΔG_{lipo}	^e ΔG_{solvGB}	^f ΔG_{vdw}
1	-53.49	-19.71	11.21	-1.1	-15.94	16.16	-41.6

2	-60.11	-24.26	2.6	-3.11	-16.72	21.41	-38.06
3	-57.42	-30.75	11.19	-2.46	-15.14	24.55	-42.93
4	-79.64	-67.22	15.85	-2.75	-25.23	49.3	-48.34
5	-92.2	-56.01	8.81	-2.81	-24.24	43.22	-61.03
6	-55.88	-23.36	9.49	-1.61	-21.91	34.61	-45.61
7	-68.38	-62.77	11.4	-2.9	-20.76	48.97	-43.29
8	-43.18	-20.38	9.68	-2.05	-19	34.7	-45.38
9	-56.58	-36.83	8.16	-2.43	-17.54	27.06	-31.14
10	-56.07	-29.68	-1.62	-2.95	-12.01	20.83	-30.35
11	-66.39	-14.76	11.63	-2.4	-19.86	13.37	-51.88
12	-68.42	-27.05	14.9	-2.41	-26.21	31.15	-54.2
13	-75.95	-27.03	17.98	-1.43	-30.89	26.73	-57.73
14	-73.12	-20.14	9.53	-2.68	-25.34	24.76	-54.44
15	-87.69	-25.88	5.43	-1.44	-32.2	30.03	-61.62
16	-74.19	-36.21	4.43	-3.44	-22.58	32.65	-47.16
17	-74.58	-10.2	-0.82	-2.74	-22.32	15.22	-51.28
18	-76.46	-37.23	5.09	-2.59	-26.68	34.65	-47.79
19	-76.12	-11.02	10.29	-2.33	-26.48	19.04	-61.4
20	-82.12	-47.98	8.04	-3.79	-28.01	45.45	-55.12
21	-73.34	-33.07	11.38	-1.49	-28.26	33.1	-53.99
22	-75.48	-24.53	7.92	-1.43	-27.22	28.42	-57.27

23	-59.96	-0.8	3.32	-1.89	-18.72	15.9	-54.77
24	-56.43	-19.33	2.8	-0.43	-15.24	18.62	-42.77
25	-57.81	-37.06	9.08	-3.09	-17.83	30.28	-38.62
26	-50.35	-22.95	2.55	-2.02	-11.24	20.24	-37.09
27	-71.31	-45.56	2.47	-2.77	-24.08	36.33	-36.41
28	-51.03	-14.49	4.35	-1.18	-14.84	20.78	-43.51
29	-63.5	-5.95	6.4	-1.21	-17.81	15.71	-58.99
30	-61.92	-13.67	9.8	-1.08	-18.32	14.85	-51.78
31	-69.54	-57.1	14.58	-3.36	-16.03	32	-39.49
32	-64.85	-11.15	5.42	0.26	-26.68	21.55	-52.5
33	-56.83	-12.27	11.2	-0.9	-19.92	19.44	-52.29
34	-67.88	-15.53	4.92	-1.68	-20.73	5.59	-36.64
35	-66.57	-6.48	14.88	-0.14	-24.71	18.44	-66.3
36	-80.78	-45.16	12.37	-2.42	-25.77	41.47	-60.47
37	-75.33	-16.72	12.61	-1.92	-30.73	25.88	-62.76
38	-81.97	-15.48	10.13	-1.86	-25.21	7.17	-54.91
39	-67.36	-19.01	3.57	-0.52	-26.26	26.76	-50.23
40	-54.54	-18.38	10.51	-0.36	-26.85	27.28	-45.29
41	-66.97	-34.67	2.71	-1.41	-27.41	35.01	-39.62
42	-57.05	-13.89	7.41	-1.25	-25.36	21.71	-45.67
43	-67.58	-59.98	6.66	-1.56	-25.09	55.7	-43.76

44	-72.78	-17.06	4.76	-0.89	-27.94	21.55	-51.73
45	-64.88	-11.91	8.1	-1	-27.96	26.76	-58.1
46	-59.6	-6.22	-2.6	0.49	-27.48	25.64	-48.77
47	-69.38	-29.71	11.61	-0.65	-29.63	31.42	-49.53
48	-63.49	-34.39	11.03	-2.08	-27.26	36.43	-45.02
49	-72.69	-34.96	8.63	-1.16	-28.35	33.15	-48.79
50	-69.8	-21.03	3.77	-0.59	-27.73	29.32	-51.85
51	-60.66	-12.71	3.72	-0.52	-25.88	27.05	-50.98
52	-65.21	-21.74	4.74	-0.98	-27.12	30.31	-49.03
53	-65.12	-5.59	3.99	-0.06	-27.83	17.33	-51.37
54	-60.69	-16.38	6	-0.84	-26.48	28.4	-51.18
55	-67.88	-28.43	4.94	-0.72	-27.6	32.03	-46.73
56	-73.3	-29.17	5.01	-1.03	-27.99	30.03	-48.65
57	-75.4	-29.22	5.01	-1.96	-25.4	25.3	-48.48
58	-67.12	-21.17	11.41	-0.68	-24.95	27.56	-54.82
59	-70.74	-29.72	8.91	-1.79	-25.15	33.16	-53.16
60	-80.37	-44.57	9.85	-3.15	-25.64	39.43	-53.7
61	-80.39	-28.29	8.15	-2.19	-25.79	27.69	-56.98
62	-42.23	-22.74	7.06	-2.37	-16.27	30.71	-35.64
63	-64.96	-19.14	12.19	-2.14	-27.63	29.23	-54.91
64	-47.56	-17.52	3.41	-2.41	-18.8	28.63	-41.43

65	-62.76	-21.2	8.11	-2.06	-23.71	24.32	-48.11
66	-75.51	-38.71	10.06	-1.79	-27.38	39.17	-54.27
67	-62.53	-24.47	8.44	-2.43	-22.32	29.21	-50.62

^aFree energy of binding; ^bCoulomb energy; ^cCovalent energy (internal energy); ^dhydrogen bonding energy; ^ehydrophobic energy (nonpolar contribution estimated by solvent accessible surface area); ^felectrostatic solvation energy; ^gvan der Waals energy.

Table S7. Count and percentage of actives in top N% of decoy results.

% Decoys	1 %	2 %	5 %	10 %	20 %
# Actives	7	7	7	7	7
% Actives	70.0	70.0	70.0	70.0	70.0

Table S8. Count and percentage of actives in top N% of results.

% Results	1 %	2 %	5 %	10 %	20 %
# Actives	7	7	7	7	7
% Actives	70.0	70.0	70.0	70.0	70.0

Table S9. Enrichment Factors with respect to N% sample sizes.

% Samples	1 %	2 %	5 %	10 %	20 %
EF	71	35	14	7	3.5
EF*	70	35	14	7	3.5

EF'	1.3e+02	67	27	14	7
EFF	0.972	0.944	0.867	0.75	0.556

EF: Enrichment factor (Number of ranked results for which to calculate the enrichment factor);

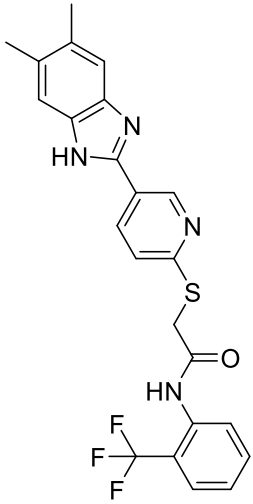
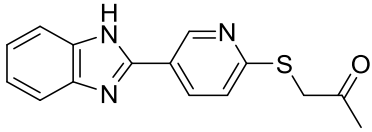
EF*: Enrichment factor (Number of ranked decoys for which to calculate the enrichment

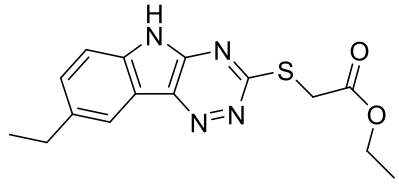
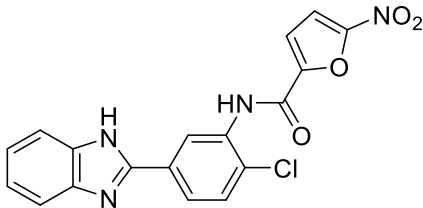
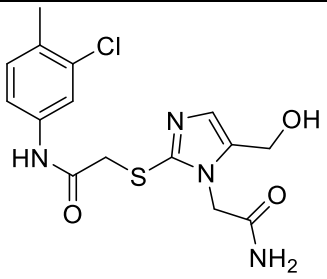
factor); EF': Enrichment factor Prime; EFF: Active recovery Efficiency.

Table S10. Hydrogen bond occupancy compound 5/5I12 complex.

Amino acid residue	Hydrogen bond occupancy (%)
Tyr179	56%
Leu188	72%
Ala189	79%
His190	46%
His191	49%
Phe192	39%
Glu227	25%

Table S11. Table showing docking results, binding free energy (kcal/mol) and predicted activity of pharmacophore generated virtual hits in the catalytic pocket of MMP-9 enzyme (PDB:5I12).

Title	Compound	^a G _{score}	^b ΔG _{bind}	Predicted activity	Molecular Properties				
					^c M.W	^d SASA	^e DonorHB	^f AcceptHB	^g LogP _{o/w}
CACPD2011a-0002144822		-10.967	-68.65	7.963	456.485	766.666	2.000	5.000	5.789
CACPD2011a-0000241403		-9.948	-62.97	7.562	283.347	559.609	1.000	4.500	2.969

CACPD2011a-0000542004		-9.642	-59.63	7.589	316.377	619.899	1.000	5.000	2.994
CACPD2011a-0001461212		-9.685	-55.76	6.825	382.762	647.010	2.000	5.500	3.069
CACPD2011a-0000963808		-9.56	-42.29	6.845	368.837	650.274	4.000	8.200	0.946

^aglide score; ^bFree energy of binding; ^cM.W: Molecular Weight; ^dSASA: Solvent accessible surface area (300-1000); ^eDonorHB: Total number of hydrogen bonds of the molecules that are to be donated to water molecules of solvent (0.0-6.0); ^fAcceptorHB: Total number of hydrogen bonds of the ligands to be accepted by from the water molecules of solvent (2.0-20.0); ^gQPLogP_{O/W}: Predicted octanol/water partition coefficient (-2 to 6.5).

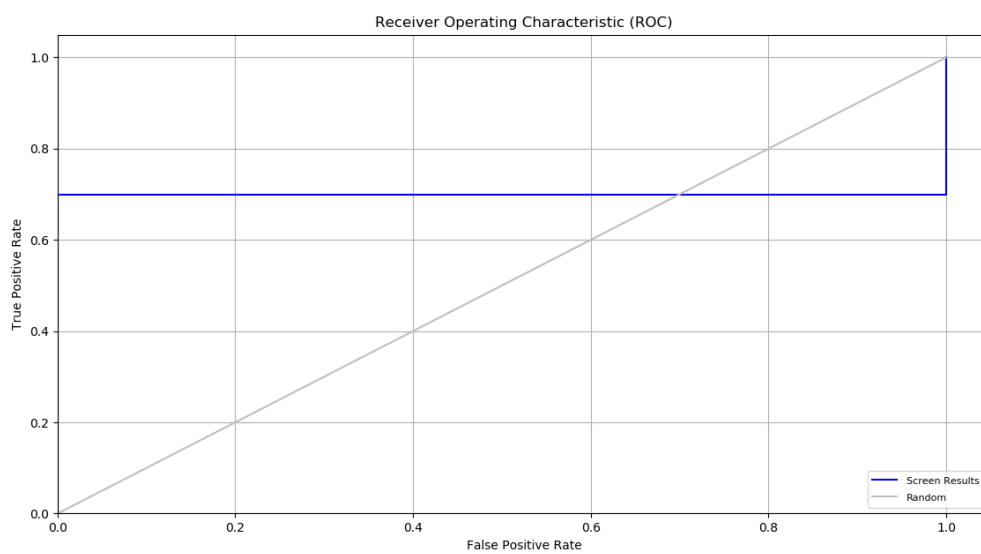


Figure S1. ROC curve obtained by DDHRR_1 model against randomly curve.

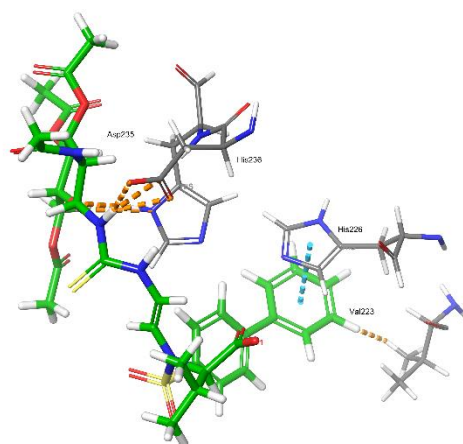


Figure S2. Represents three-dimensional diagram of cocystal/5I12 complex

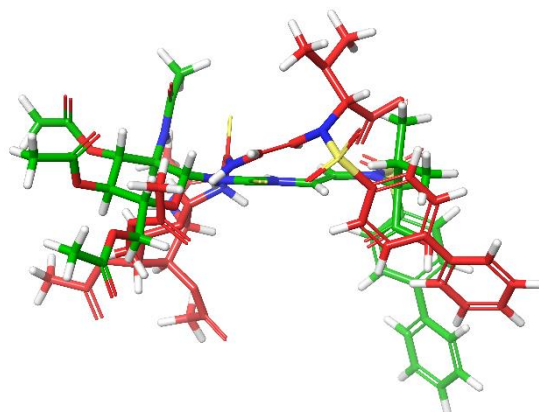


Figure S3. Represents superposition of conformations of cocystal (red) and best XP-docking pose (Green)

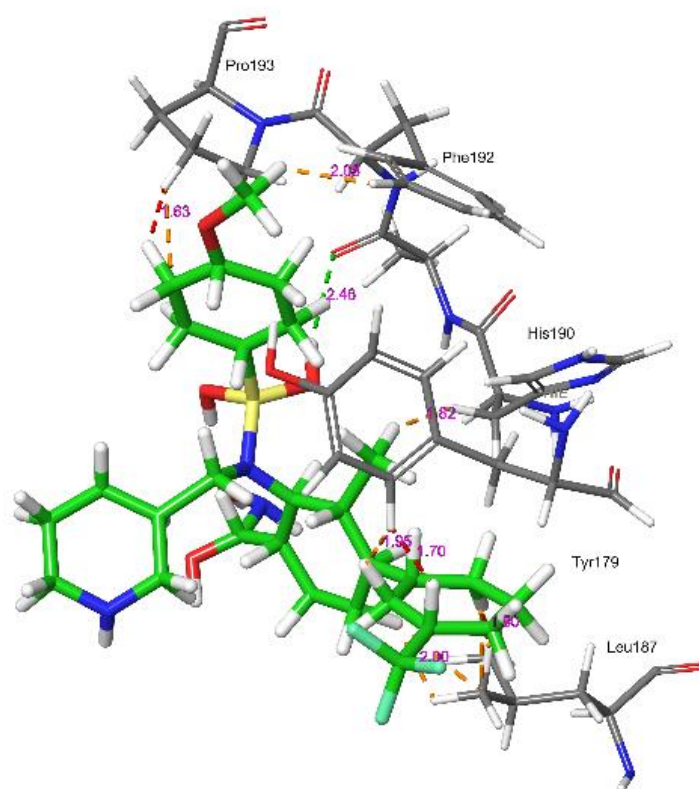


Figure S4. Represents three-dimensional diagram of compound 5/5I12 complex

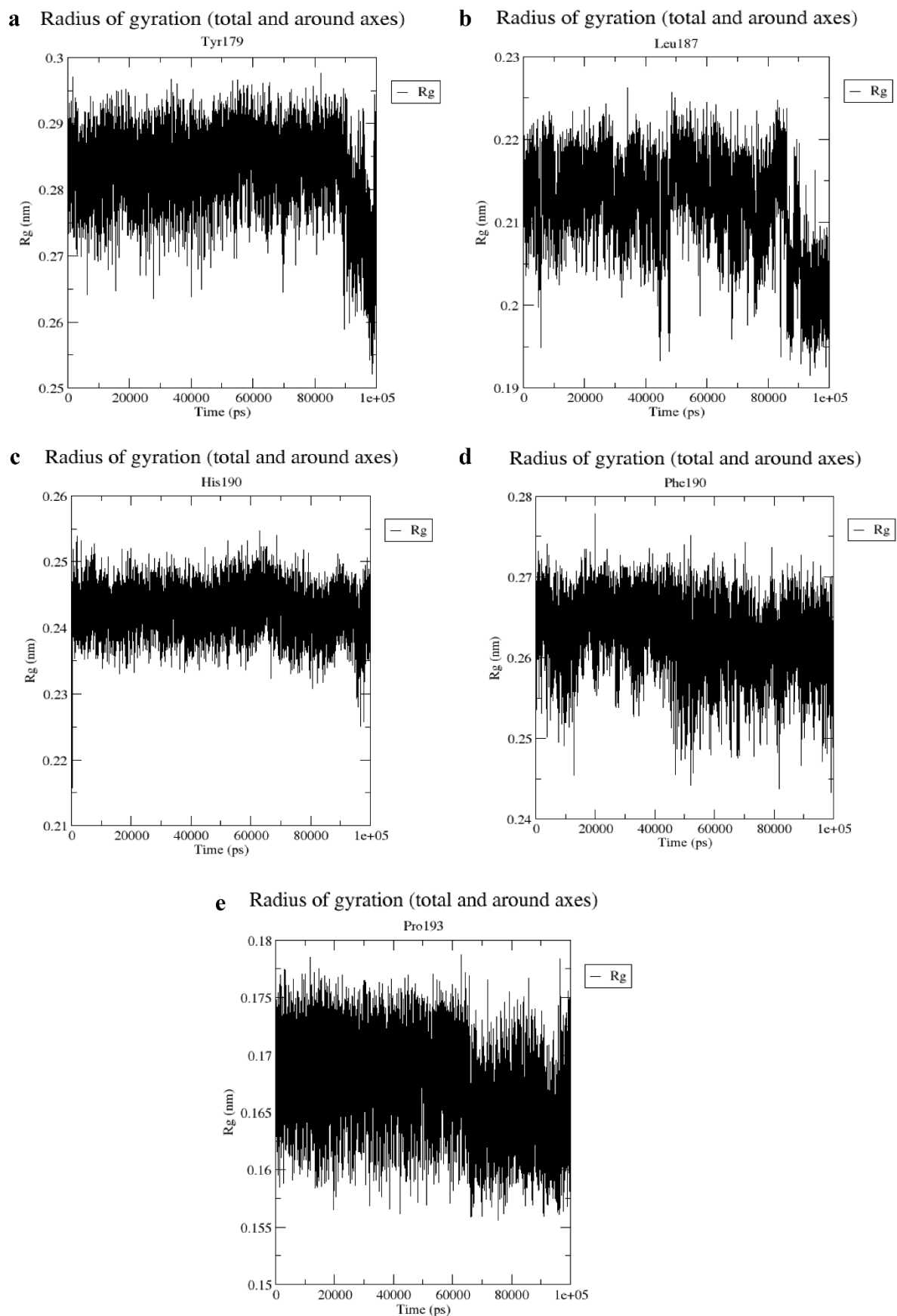


Figure S5. Radius of gyration of (a) Tyr179 (b) Leu187 (c) His190 (d) Phe192 (e) Pro193 5/5I12 complex for 100 ns MD simulation trajectory

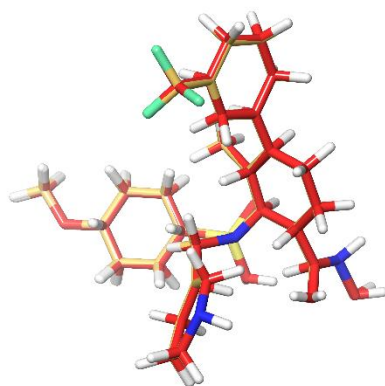


Figure S6. Represents superposition of **5** snapshots at 10 ns intervals from the 50 ns MD simulation trajectory.

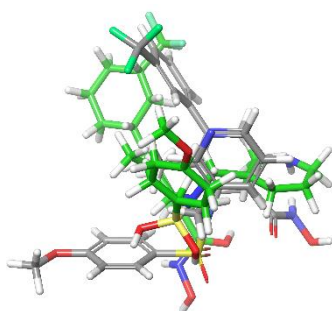


Figure S7. Represents superposition of conformations of inhibitor **5** after MD simulation (Green) and best XP- docking pose (Grey)

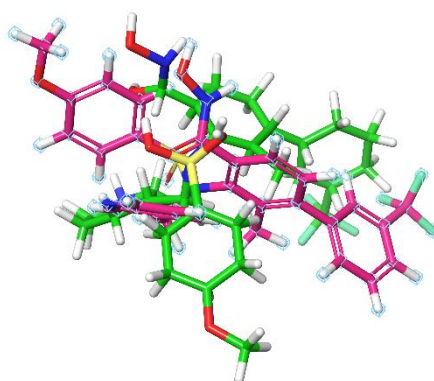


Figure S8. Represents superposition of conformations of inhibitor **5** after MD simulation (Green) and pose of the pharmacophore model (Pink)

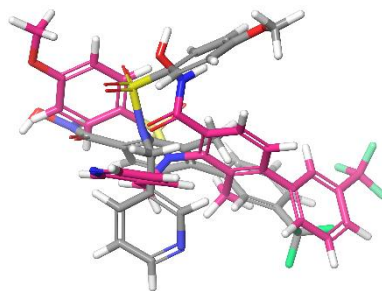


Figure S9. Represents superposition of conformations of inhibitor **5** best XP- docking pose (Grey) and pose of the pharmacophore model (Pink)

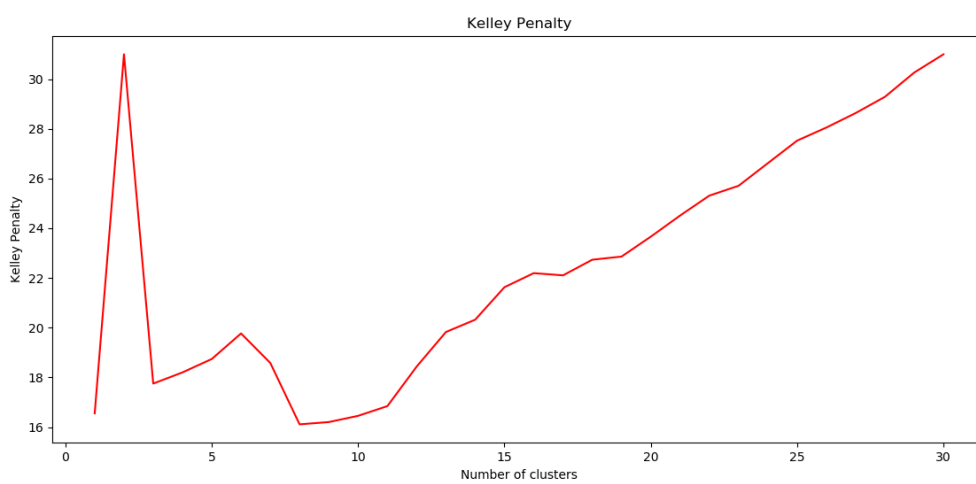


Figure S10. Represents a Kelley penalty plot against number of clusters.

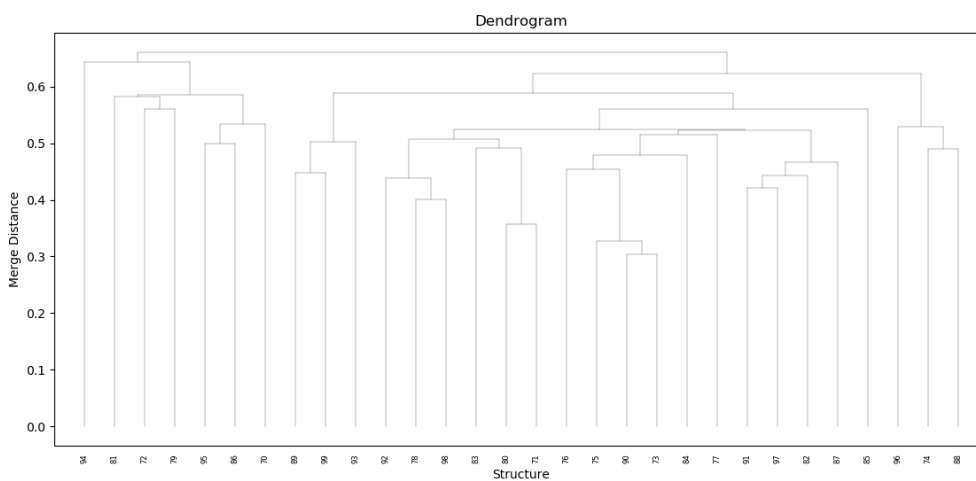


Figure S11. A dendrogram representing merging distances with reference to the cluster indices.

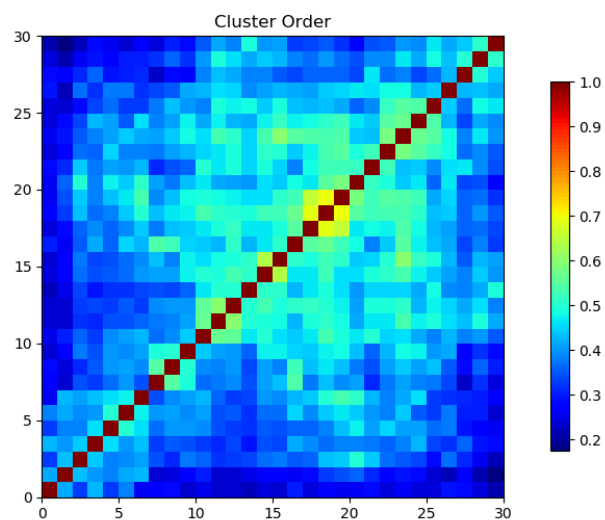


Figure S12. A distance matrix plot showing the dissimilarity between the clusters based on cluster order.

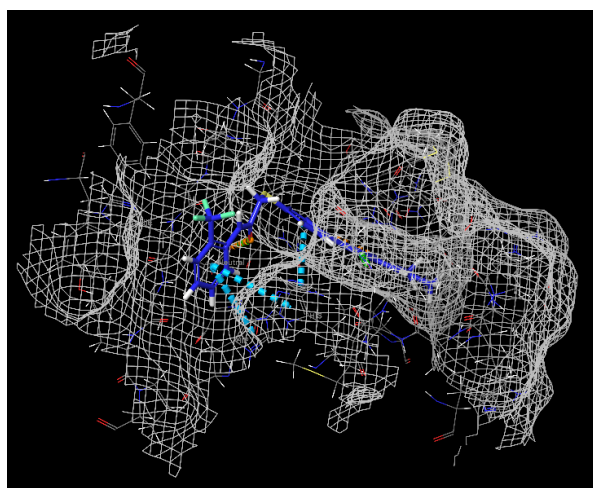


Figure S13. 3-dimensional diagram of virtual hit VH1 pose within the catalytic pocket of 5I12.

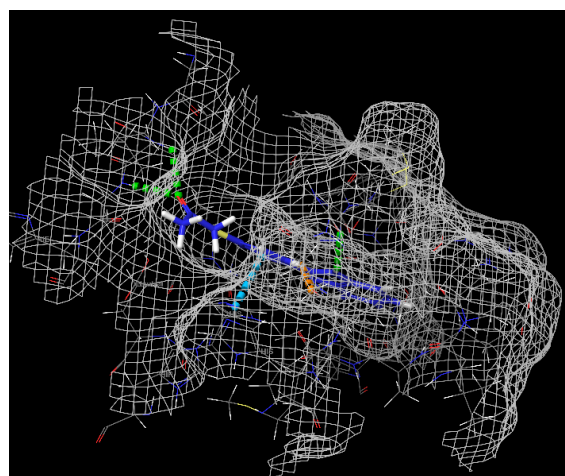


Figure S14. 3-dimensional diagram of virtual hit VH2 pose within the catalytic pocket of 5I12.

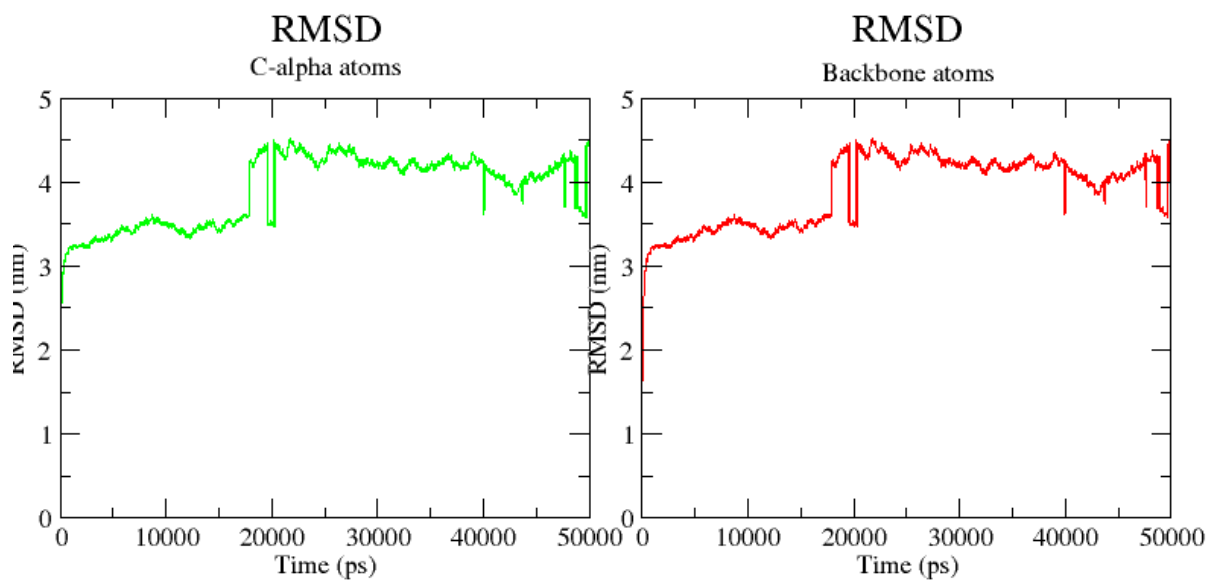


Figure S15. Represents RMSD (\AA) of (a) $C\alpha$ atoms of protein from those in initial structure (b) protein backbone from the initial structure of complex VH1/5I12 during MD simulation.

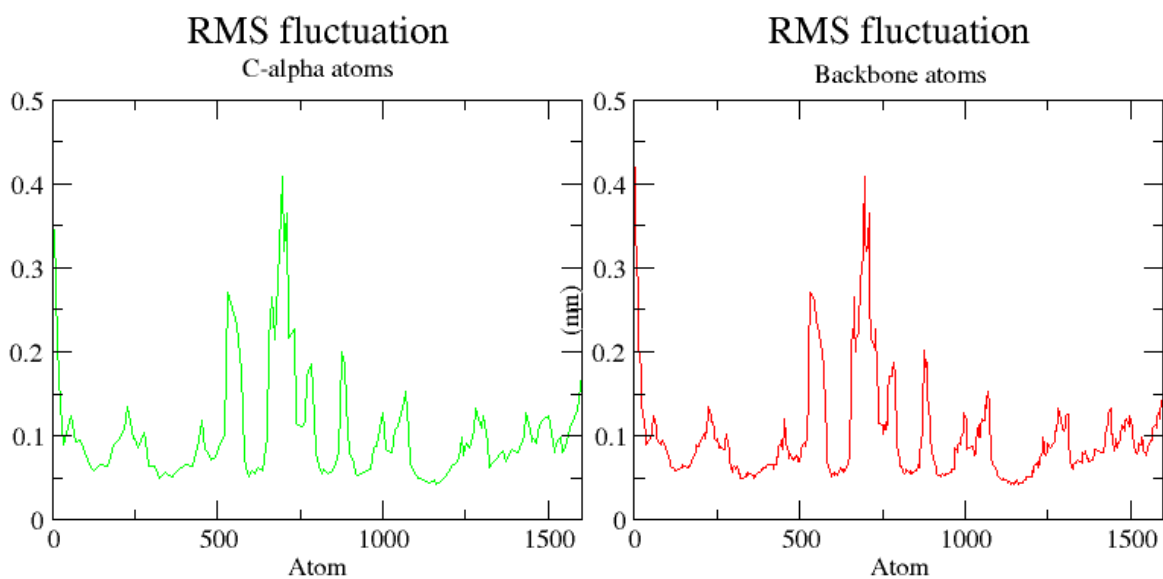


Figure S16. Represents RMSF (\AA) of (a) $C\alpha$ atoms of protein from those in initial structure (b) protein backbone from the initial structure of complex VH1/5I12 during MD simulation.

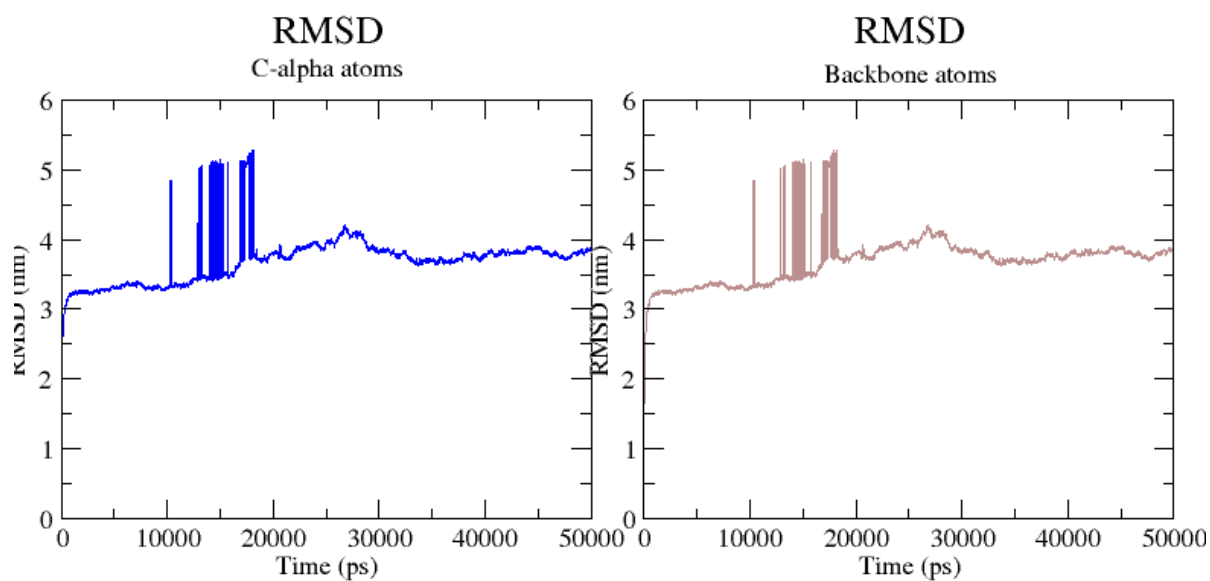


Figure S17. Represents RMSD (\AA) of (a) $C\alpha$ atoms of protein from those in initial structure (b) protein backbone from the initial structure of complex VH2/5I12 during MD simulation.

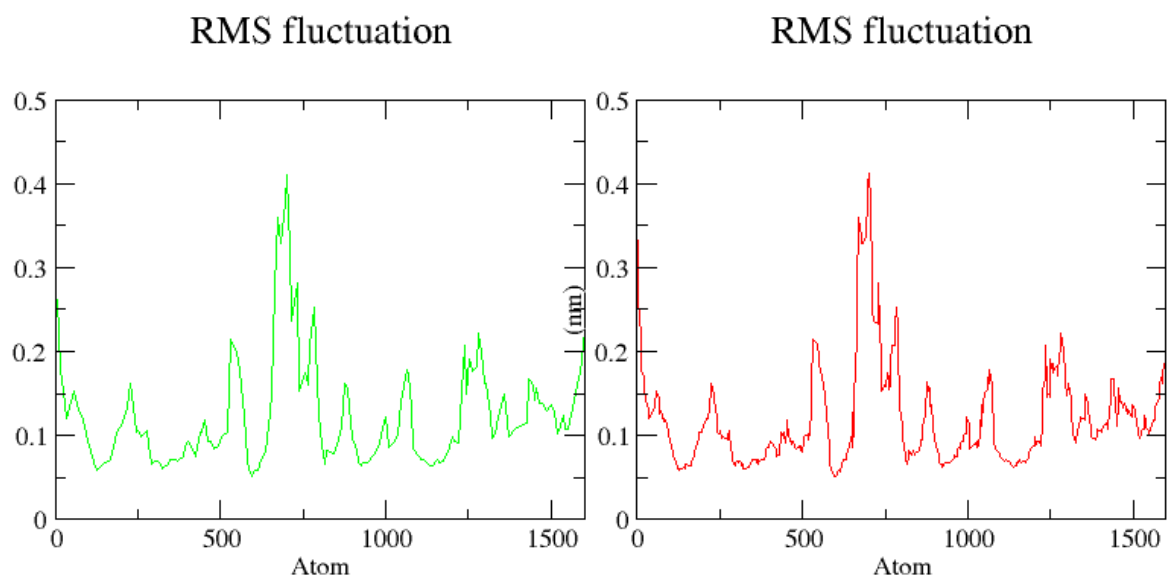


Figure S18. Represents RMSF (\AA) of (a) $C\alpha$ atoms of protein from those in initial structure (b) protein backbone from the initial structure of complex VH2/5I12 during MD simulation.